This is to certify that the

thesis entitled

SURFACE MORPHOLOGY OF GLASS CAPILLARIES
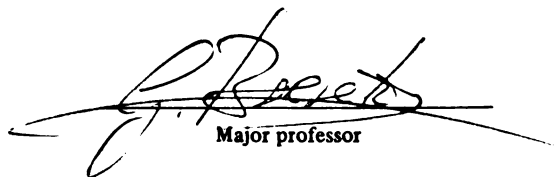
presented by

Jakob LaVerne Steffey

has been accepted towards fulfillment
of the requirements for
M.S.   Mechanical
_____ degree in ___Engineering___

_____
Major professor

Date 30th September 2002

PLACE IN RETURN BOX to remove this checkout from your record.
TO AVOID FINES return on or before date due.
MAY BE RECALLED with earlier due date if requested.

DATE DUE	DATE DUE	DATE DUE

SURFACE MORPHOLOGY OF GLASS CAPILLARIES

By

Jakob LaVerne Steffey

A THESIS

Submitted to
Michigan State University
in partial fulfillment of the requirements
for the degree of

MASTER OF SCIENCE

Department of Mechanical Engineering

2002

ABSTRACT

SURFACE MORPHOLOGY OF GLASS CAPILLARIES

By

Jakob LaVerne Steffey

In this work, the surface properties related to nucleation phenomena in silica glass capillary tubes are investigated. Surface topography and surface energy are theorized to play a role in heterogeneous bubble formation of super-saturated liquids and are therefore the focus of this study. Procedures for modifying and measuring properties of glass surfaces were of particular interest. Surface modification treatments involving hydrofluoric acid etching and alkylsilane derivitizations were performed. Surface data collection techniques included atomic force microscopy and solid-liquid-vapor contact angle measurements.

Techniques to successfully profile the surface of capillary tubes were defined and a novel approach was developed to interrogate the internal surface of small-diameter tubes. The roughness of capillary tube surface was modified and was measurable in a consistent manner. The research performed here should allow designing of glass surfaces to promote or inhibit bubble formation by altering the chemistry or topography of the surfaces.

ACKNOWLEDGEMENTS

TABLE OF CONTENTS

LIST OF TABLES

LIST OF FIGURES

NOMENCLATURE

D	tube diameter
f	friction factor
J	nucleation rate
k	Boltzmann constant
N_l	number of liquid molecules per unit volume
m	mass of one molecule
Re	Reynolds number
r_e	equilibrium radius
T	absolute temperature
W_{max}	maximum reversible work
Δp	pressure change
ε	equivalent roughness
ϕ	bubble shape factor (0 for pancakes, 1 for spheres)
γ_{LV}	liquid-vapor surface free energy
γ_{SL}	solid-liquid surface free energy
γ_{SV}	solid-vapor surface free energy
μ	viscosity
π	3.141592653...
θ	contact angle
ρ	density
σ	surface tension

Chapter 1

Introduction

This study is concerned with the surfaces of glass capillary tubes as they relate to nucleation and with ways of measuring and modifying those surfaces. The motivation for this study stemmed from experimental findings of raised heterogeneous nucleation thresholds for super-saturated liquids in confined volumes, paired with poor understanding of how the surface properties affect the thresholds. In particular, Liu (2001) conjectured that the surface roughness of capillary tubes might be correlated with the effect of raised nucleation thresholds. If the surface roughness of small fused silica capillary tubes is measurable, then Liu's conjecture can be tested. A relationship between capillary tube size and surface roughness would provide a factor in heterogeneous nucleation equations to better model the trends found in experimental data. Since little is known about the surface inside capillary tubes and because of the vast number of uses of capillary tubes, the surface topography is also interesting as a general topic.

1.1 Applications of Capillary Surface Science Research

Bubble formation in capillary tubes is applicable to other engineering applications that include:

-engineering of chemical processes and reactions

-predicting nucleation points in confined volumes

-designing microchannel heat exchangers

-designing miniature pumps

- improvements in experimental direct delivery of oxygen to organs of heart attack and lung disease patients

-designing of devices for emergency oxygen delivery to contaminated rivers, streams, lagoons, and waste water

-increasing aerobic activity in processing of sewage, fermentation of yeast, curdling of milk, and many other processes

1.2 Literature Review

1.2.1 Surface Measurements and Treatments

Contact angles are indicators of the attraction a liquid has for a flat solid surface. They are measurements of the angle a liquid drop makes with the solid surface, at the edge of the solid-liquid interface. Contact angle measurements are important to this study because of the way they relate to surface energy and how surface energy affects heterogeneous nucleation. Young's equation relating contact angle to surface free energy is shown in equation (2.1). Liquid-vapor interactions at solid surfaces are affected by the surface free energy, thus affecting heterogeneous nucleation phenomena. Published literature for water contact angles on glass show small angles. The surface free energy of water on silica glass is approximately 70 to 78 dynes/cm. This corresponds to contact angles between 0° and 5° (Adamson 1990). The surface free energy of water on glass derivitized with Siliclad^{TM}, a hydrophobic siloxane, as published by the manufacturer Gelest, is 31 dynes/cm, giving contact angles near 88°.

While smooth surface data are conventionally cited in reference tests, non-uniform surfaces have given lower contact angles than those of smooth surfaces, in the range of 0° to 90°. Rough surfaces have lower measured contact angles than smooth surfaces because the increased free energy of the rough surface aids in spreading the fluid across the material, see equation (2.1). In literature, surface roughness has caused air trapping during contact angle measurement, creating a composite surface effect (Adamson 1990). The composite surface will affect the measured contact angle to an extent determined by the ratio of the composite areas and their physical properties (Adamson 1990).

Roughening of silica glass is of interest to this study because of the effects surface roughness has on nucleation thresholds and how they can be controlled through surface manipulation. A technique for roughening silica glasses is etching with hydrofluoric acid. Little research has been published involving measurement of the roughening effect of etching silica glass surfaces. Affatigato et al (1996) reported on how the initial surface roughness of glass affects subsequent etching. They found that etching of abraded silica surfaces causes initial flaws to deepen quickly, while growing laterally at a slower pace (Affatigato et al 1996). The lateral growth reduces the flaw concentration and causes local surface slopes to become gentler, decreasing the surface area of the glass sample. For the first ten minutes of etching, all of the abraded glass samples were found to quickly increase in root-mean-square (RMS) roughness at a rate in proportion to the effective surface area of their abraded surface (Affatigato et al

1996). The roughness of the coarsely abraded glass slowly reduced in RMS roughness, and the finely abraded glass slowly increased in RMS roughness, after the initial 10 minutes of etching. Data from Tso et al (1982) and Spierings (1993) also support the observations of Affatigato et al (1996). Unfortunately, the etched glass data from literature cannot be directly compared with the results of this study. The experiments in the literature used several orders of magnitude rougher surfaces and larger sample areas than used in this study, reducing the usefulness of comparisons to trends in roughness and topography.

A potential method of measuring the surface roughness of glass capillary tubes is through the recovery of the roughness contribution to the pressure drop of a turbulent fluid flow through the tube. Due to the scarcity of data relating fluid flow rates through capillary tubes to the capillary tube roughness, generalized pipe flow theory is presented and discussed here. Flow rates of fluids through pipes has been a topic covered in fluid dynamics literature for several decades. Flow rates are governed by fluid viscosity, fluid density, pressure drop, pipe diameter, pipe length, and roughness of the pipe wall. It is convenient to relate pressure drops and flow rates using a friction factor, equation (1.1). For laminar Newtonian flows, the Darcy friction factor of 64 divided by the Reynolds number gives the exact friction induced by the fluid-wall boundary, regardless of the wall roughness. The friction factor is derived using the Newtonian relation between shear stress and fluid velocity gradient and only depends on the Reynolds number in laminar flow. In turbulent flows, the friction factor becomes much more complex than for laminar flows. With turbulent flows, models such as the

4

Colebrook formula, equation (1.2), can be used to describe the dependence of friction factor on Reynolds number, equation (1.3), and the wall roughness. Thus if the friction factor, the pipe diameter, and the Reynolds number are determined, the roughness, ε, can be found from equation (1.2).

$$\Delta p = f \frac{l}{D} \frac{\rho V^2}{2}$$
(1.1)

$$\frac{1}{\sqrt{f}} = -2\log(\frac{\varepsilon/D}{3.7} + \frac{2.51}{Re\sqrt{f}})$$
(1.2)

$$Re = \rho VD/\mu$$
(1.3)

The Colebrook formula has limitations, since it is an empirical fit of pressure drop and flow rate data versus pipe surface roughness data. As a rule of thumb a 10% error in the friction factor is the best expected (Munson et al 1998). In extreme cases, such as very smooth or very rough surfaces, or Reynolds numbers near the transition region, the Colebrook formula can produce much larger error. For very smooth surfaces, nearly all of the frictional drag comes from the molecular interactions of the fluid and the wall. The no-slip boundary condition plays a major role in the shear force on the liquid flow, especially when the equivalent roughness of the pipe walls is considerably smaller than the viscous sublayer thickness (Munson et al 1998). Such pipes are called hydraulically smooth. Roughness calculations for hydraulically smooth pipes should not be performed using experimental data and the Colebrook formula, since extremely large error can arise. A 0.5% drag increase from the

nanoscale roughness of a pipe wall, added to the no-slip boundary shear drag, would not be determinable when a few percent error in the Colebrook formula or data collection is present. Error in data collection can come from flow volume, time, pipe length, and pressure measurements. Error can also arise from abnormally shaped pipe entrances, most significantly affecting the pressure loss and flow rate through short pipes.

1.2.2 Nucleation Theory

Current nucleation theories are essentially empirical models that attempt to relate nucleation rate to the energy of the molecules of the nucleating species. There are nucleation rate theories for homogeneous and heterogeneous nucleation events. Equation (1.4) is an example of classical homogeneous nucleation theory (Carey 1992).

$$J = N_l \sqrt{\frac{3\sigma}{m\pi}} \exp\{-W_{max}/(kT)\} \qquad (1.4)$$

Heterogeneous nucleation theory is more complex because nucleation typically takes place at preferred sites on surfaces where the topology and surface chemistry favor nucleation. The heterogeneous equations are empirical modifications to homogeneous nucleation theories. They are difficult to test and verify because of the difficulty in measuring true nucleation rates. Heterogeneous nucleation theory is complicated by the properties of the liquid and the material surface, trapped gases in crevices, and impurities. Equation

6

(1.5) is given as an example of a heterogeneous nucleation rate equation with a bubble shape factor (Liu 2001). The bubble shape factor allows for modeling the effect that bubble growth in crevices has on nucleation behavior.

$$J = N_l^{2/3} \sqrt{\frac{3\sigma}{m\pi}} \exp\{-\frac{4}{3}\varphi\pi r_e^2 / (kT)\}$$

(1.5)

1.2.3 Nucleation in Confined Volumes

Nucleation of liquids in microchannels (< 1 mm width) has been a topic of recent research in the heat transfer field. Electronic devices are becoming smaller and more powerful, requiring high heat fluxes through small areas to keep them at operating temperatures. Researchers have slowly gathered physical data related to microchannel heat exchangers and have been trying to manipulate the governing thermodynamic equations to match the newly acquired physical data (Peng et al 2001). The data in this field are very sparse, and the equations relating nucleation to superheat and microchannel size predict much higher superheats than has been observed in capillary tube experiments of the same nature (Brereton et al 1998).

Though the data are sparse in the microchannel research field, the researchers have introduced confined volume nucleation-related phenomena not observed in other research fields. Two new terms have recently been defined by microchannel researchers; fictitious boiling and evaporating space. Fictitious boiling refers to oscillations of the fluid flow in micro-channels, at temperatures or heat fluxes just below the critical values where nucleate bubbles will form and grow. Rapid nucleate formation and extinction along the microchannel possibly

cause fictitious boiling. Liquid in the fictitious boiling regime has been observed to absorb much more heat than the normal liquid sensible heat, resulting in very high heat transfer rates. These rates may even exceed that of nucleate boiling in macrochannels (Peng et al 1998).

Evaporating space is the volume required for nucleate embryos to grow and form bubbles. Normal bubbles can only form if the liquid expansion space is greater than the critical value. Bubble embryos can still form in spaces smaller than the evaporating space, however, since their size cannot grow up to the critical bubble radius formulated by conventional nucleation theory, they must eventually collapse. Rapid and continuous bubble nucleate growth and collapse is called fictitious boiling, mentioned previously (Peng et al 2001).

In one case, Peng et al (1998) created a phase stability criterion derived from classical thermodynamics, the Clausius-Clapeyron equation, and entropy change of a nucleate bubble due to heat flux through a micro-channel wall. The criterion allows prediction of the heat flux required for pure liquids to nucleate in microchannels, although there are few data that supports it. The criterion requires assumptions that the heat diffusion only occurs in the vapor phase because the nucleate embryo is assumed to occupy most of the microchannel. These two connected assumptions are part of the reason why the stability criterion has not held up in more recent findings (Peng et al 2001), although it is always difficult to model a dynamic system accurately without proper correction factors for all the dynamic tendencies of the system.

In a subsequent work, Peng et al (2001) demonstrated that the existence of external perturbations could largely depress the size of embryos and yield fictitious boiling in liquids. An impulse pressure wave generated from the emergence of embryos reflected back to the embryos, off the confining micro-channel wall, was theorized to collapse the embryo (Pang et al 2001). The field of microchannel research appears to be much more complex than has been introduced so in literature. Pang's (2001) predicted data trends are qualitatively correct, although proposed confined volume nucleation models do not fit known physical data well. Some experimentally determined nucleation points are half the superheat temperatures that would be expected by the calculations from the microchannel researchers. However no account is made of the surface topologies in these studies, and the extent to which it influences the results and observations is not known. Also, the fluid was not pre-compressed in Pang's experiments, which may lower the measured nucleation thresholds by providing nucleation sites of undissolved gas nuclei on the microchannel surface (Brereton et al 1998).

Brereton et al (1998) determined nucleation thresholds of pre-compressed water supersaturated with oxygen in capillary tubes of inside diameter less than 200 μm and measured the superheat at which pure water nucleates in capillary tubes of inside diameter between 15 and 150 μm. A dual-dependence model was calibrated to agree well with the experimental data, though no factors were included in the model to account for the differing surface properties among the different diameter capillary tubes. Determining the surface properties of capillary

tubes may provide more information about how to improve heterogeneous nucleation models from a better understanding of the system kinematics.

1.2.4 Particle Adhesion and Contamination

Contamination of surfaces is a major concern in surface science research, particularly when surface cleaning or preparation is considered, or real surface topologies are to be measured. Contaminants can severely affect measurement of the chemical and physical properties of surfaces. For example, there has long been a question as to whether gold has a very high or very low contact angle. The present consensus is that gold is completely wetted by water (low contact angle) and earlier publications that have stated otherwise are now believed to show the ease with which surface contamination can occur (Adamson 1990).

Contamination and particle adhesion are of particular interest in capillary tube surface research. In particular, parts of the tube wall must usually be ground away to expose the inner surface of the capillary tube before data from the inner wall can be acquired. Exposure of the inside of silica glass capillaries requires glass removal by any of numerous methods. Glass removal processes include etching, grinding, polishing, scrubbing, and fracturing. Of these methods, chemical etching is an unreasonable candidate because of its slow removal rate and the unavoidable presence of vapors that etch and alter the inside capillary tube surface. The remaining glass removal processes are mechanical methods, which tend to produce glass debris and contaminate the inside of the capillary tubes. A reduction of surface contamination may come from mechanical material

removal processes paired with fluid flow to help flush the waste material away and reduce surface contamination. When a nearly contaminate free surface is necessary, improved processes of glass removal, or particle removal techniques may be required.

Ghosh and Ryszytiwskyj reviewed literature pertaining to removal of glass particles from glass surfaces (Ghosh et al 1992). They covered various methods of surface contaminate removal, although all the methods of debris removal, except chemical etching, were stated to work only for 0.2 micron or larger size particles. Since there are no known techniques to remove nanoscale particles without altering the surface topography, it is most straightforward to avoid any contamination of glass surface during preparation.

1.3   Goals and Objectives

In light of the literature discussed above, there is a clear need to quantify the topography of the surfaces involved in nucleation experiments and correlate surface characteristics with their thermodynamic properties. Therefore, an important goal of this research was to quantify the roughness of silica capillaries. A more general objective of this study was to determine testing methods for measurement of surface properties in capillary tubes.

Another objective was to characterize the effects of surface treatments of capillary tubes. Treatments that alter the surface chemistry and topography of silica glass were of particular interest because of their application in the investigation of the dependence of nucleation phenomena on surface properties.

Chapter 2

Experimental Procedures

It was hypothesized that flat glass surfaces would be easier to measure and modify than surfaces inside capillary tubes. Therefore, preliminary measurements of surface characteristics were performed on slide glass. The results provided guides to designing procedures for surface treatments of capillary tubes. The more pertinent experiments involving modifications and measurements inside capillary tubes were then carried out. Later studies will be conducted to determine the effects the surface modifications have on nucleation thresholds.

2.1   Surface Treatments of Glass

Commercial pre-cleaned glass slides (VWR Scientific Co.) were used as the medium on which the effects of several surface treatments to surface free energy and surface roughness were determined. The surface treatments used were chemical etching with hydrofluoric acid and derivitizing the surface with a hydrophobic silane solution. Table 2.1 shows the chemical treatments and duration.

Table 2.1   Glass slide treatment and duration

Treatment	Time (minutes)
no treatment	-
5% hydrofluoric acid	2
5% hydrofluoric acid	4
5% hydrofluoric acid	8
5% hydrofluoric acid	10
5% hydrofluoric acid	12
5% hydrofluoric acid	15
5% hydrofluoric acid	25
5% hydrofluoric acid	28
5% hydrofluoric acid	60
5% hydrofluoric acid	90
0.2% silane solution	0.15

During etching, the silica glass samples were suspended by their edges in 5% hydrofluoric acid. A magnetic stirrer mixed the solution at approximately 4 revolutions per second in a 500 ml Nalgene beaker. Immediately after etching, the samples were thoroughly rinsed with de-ionized water prior to a thorough rinse with acetone. The glass samples gently agitated in the silane solution were thoroughly rinsed with de-ionized water and aside for 24 hours to ensure complete reaction and adequate drying.

Due to size constraints of the Digital Instrument atomic force microscope (AFM) used in this experimentation, the pre-treated slides were cut into 10x10x1.2mm samples. Immediately after cutting with a diamond tip blade under a water jet, the glass slides were dipped briefly (1-2 seconds) in 3% hydrofluoric acid. The slides were then thoroughly rinsed with de-ionized water and acetone. The reason for this procedure was that initial AFM testing of several slides that were not dipped in HF showed contamination visible as particles of <1 μm on the

surface. Later testing of slides treated with 5% hydrofluoric acid for longer duration showed only minor changes in the surface properties of the glass for short duration initial exposure. The benefit of contamination removal was determined to outweigh the slight etching of the silica glass surface during the initial rinse after cutting.

2.2   Surface Energy Measurements

A video contact angle measurement device was used to determine the solid-liquid interface contact angle of glass slides with the surface treatments mentioned in section 2.1. A software based three-point angle approximation was used to calculate the contact angles of de-ionized water with the glass surface. A five-point calculation was also available for advancing and receding contact angles, Figure 2.1. The advancing and receding contact angles were not calculated because of difficulties with large variations in surface energy across hydrofluoric acid treated glass slides. The surface energy variations produced non-circular sessile drops and indistinguishable phase lines, as shown in Figure 2.2, introducing large variations of contact angle around single sessile drops and error from approximating the contact lines.
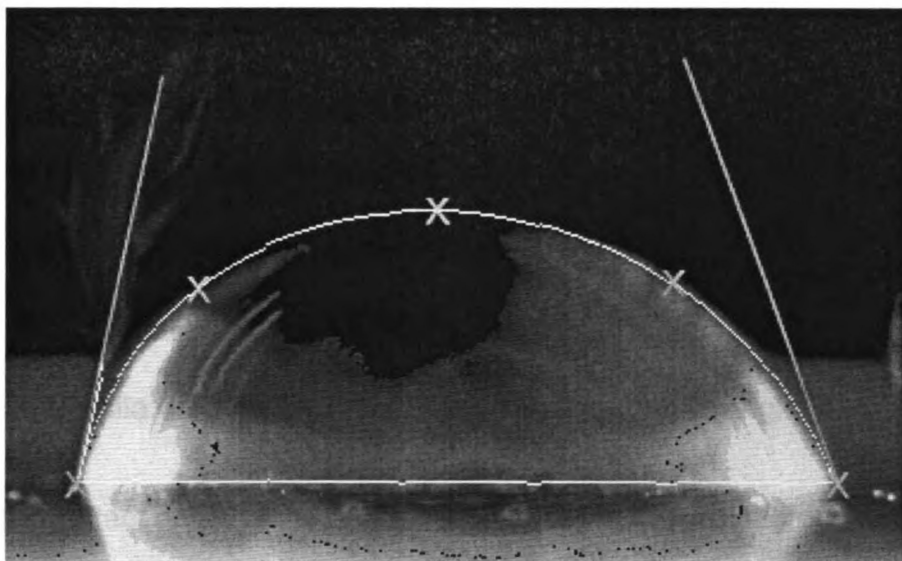
Figure 2.1 Five-point advancing and receding contact angle measurement on a hydrophobic silane derivitzed glass surface
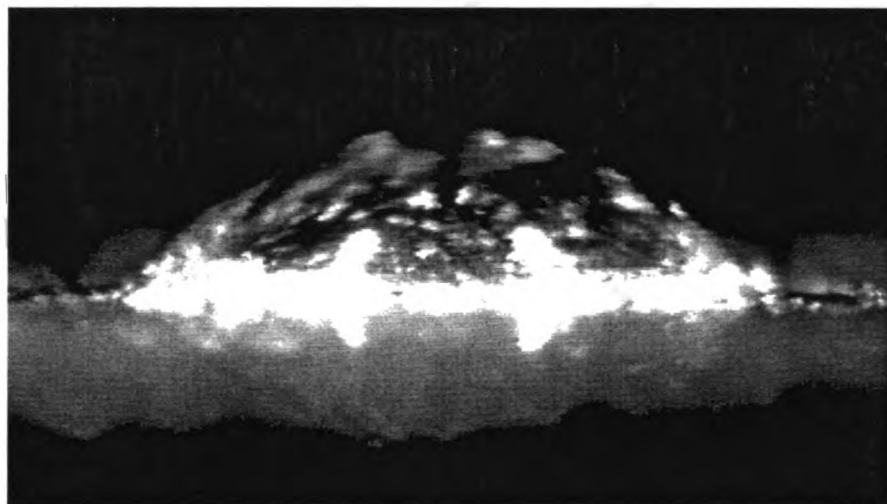

Figure 2.2 Sessile drop of water on silica with high surface energy variation
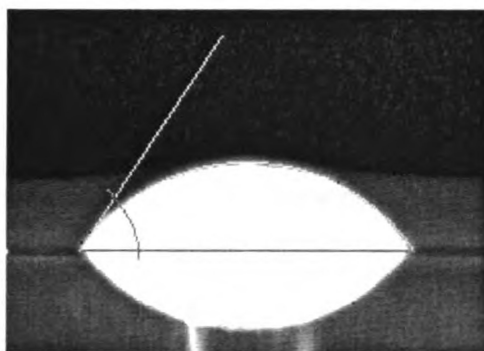
Figure 2.3 Sessile drop showing solid-liquid-vapor contact angle

The contact angle is the angle between the solid-liquid interface and the liquid-vapor interface at a three-phase point, Figure 2.3. Contact angle measurements are indicators of the available energy the glass has to attract and distribute the liquid water molecules across its surface. Figure 2.3 shows that a sessile water drop partially spreads across a silica glass surface of moderate surface energy with surface tension of approximately 60 dynes/cm. Lower surface energy of the solid results in greater beading of the water drop. Higher surface energy causes more wetting of the solid surface by the liquid. The contact angle is a measure of how well water droplets bond to the solid surface compared to how well they bond to each other. There is an equilibrium point where the surface tension of the water balances the adhesive spreading attraction of the vapor saturated solid surface. The equilibrium point is a local state of minimum energy of the solid-liquid-vapor system. Young's equation, equation (2.1), can be used to solve for the surface free energy of the silica glass, using estimates of the water surface tension (γ_{LV}) and water vapor free energy (γ_{SV}). Numerous contact angle measurements were taken for each sample to account for variations of surface properties across the surface.

$$\gamma_{SV} = \gamma_{SL} + \gamma_{LV} \cos\theta \qquad\qquad (2.1)$$

2.3 Surface Treatments of Capillary Tubes

Hydrofluoric acid treatments of silica glass capillary tubes were conducted using a syringe and connector, as shown in Figure 2.4. A 5% hydrofluoric acid solution was first drawn up the capillary tubes at an approximate rate of 0.1 milliliters per minute with a vacuum of about 12 psig. The vacuum pressure was estimated by the constant mass ratio of the volume of air at atmospheric pressure in the syringe and the volume of air under vacuum with the syringe plunger pulled back. The solution was forced out of the syringe at about 0.3 ml/min under pressure. The syringe was then replaced with another syringe containing 0.5 ml of distilled water. The distilled water was also forced through the capillary tubes at a rate of 0.3 ml/min before a final rinse of 0.3ml of acetone forced through in an identical manner from another syringe. Finally, air was forced through to remove the remaining acetone from the inside of the capillary tubes. The capillary tubes were left to dry several hours before testing proceeded.
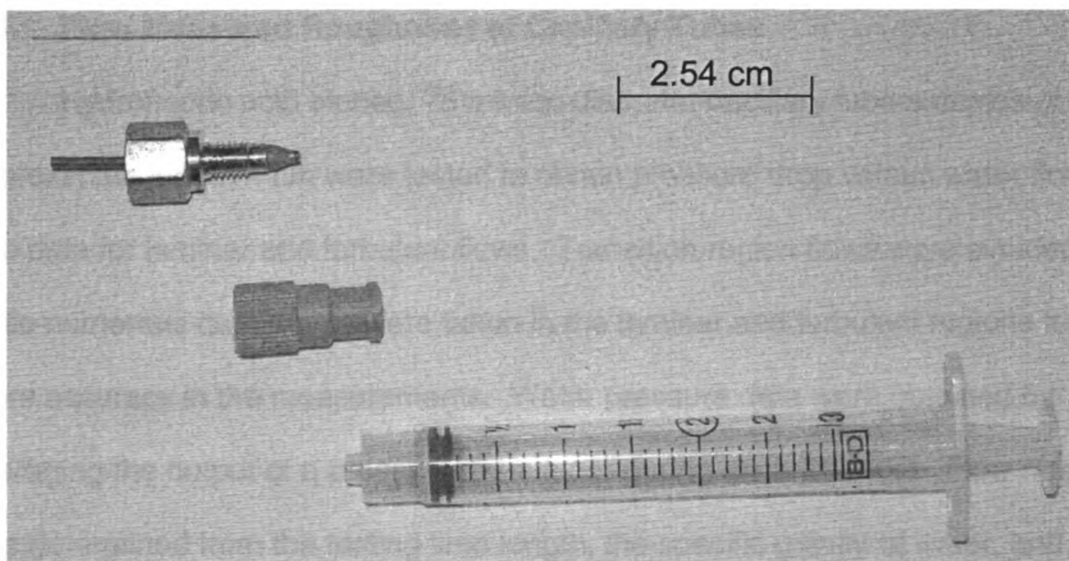
Figure 2.4 Syringe, capillary tube, and adapter

Hydrophobic silane derivatizations were performed on the capillary tube surface using a 1% solution of Siliclad™ in de-ionized water. Siliclad™ is a monomeric octadecylsilane derivative in a mixed tertiary alcohol and diacetone alcohol that reacts with water to form a silanol-rich prepolymer. The silanol-rich prepolymer condenses with available hydroxyl groups of siliceous surfaces, such as silica glass, to form a chemically bound alkylsilicone. Approximately 0.02 ml of the silane solution was forced through the capillary tubes with a syringe, allowing the solution to be in contact with the capillary walls for 10 seconds. The capillary tubes were rinsed with 0.5 ml of distilled water with a flow rate of 0.3 ml/min. The remaining water was forced out of the capillary tubes with air. The capillary tubes were then set out for a day to ensure complete reaction and adequate drying.

2.4 Flow Measured Roughness of Capillary Tubes

Hydrofluoric acid etched, 75 micron diameter capillary tube samples of approximate length 4 cm were tested to obtain pressure drop versus water flow rate data for laminar and turbulent flows. Transition region flows were avoided while numerous data points were taken in the laminar and turbulent regions for more accuracy in the measurements. Water pressure data were obtained by averaging the output of a pressure transducer during each flow test. Flow rate was determined from the testing time length, the specific gravity of water, and the weight of water collected from the flow through the capillary tube. The laminar flow data were used to determine the average diameter of each capillary tube sample with the well-established assumption that the drag force in the laminar flow region does not depend on the surface roughness of the capillary tube walls (Munson et al 1998). The turbulent flow rate data provided the necessary information for use in the Colebrook equation for estimating the roughness of capillary tube walls. The roughness data, determined for capillary tubes of different hydrofluoric acid etching times, provided an indication of the roughening effects of etching capillary tube glass. Capillary tubes of larger diameter were also tested to determine how capillary tube surface roughness depends on the capillary tube size.

2.5 AFM Profiling

Atomic force microscopy provides a method of recovering precise height profiles from movements of a small tip scanned over a surface. The tip is located

at the end of a flexible beam that allows for vertical motion of the tip, as illustrated in Figure 2.5. Table 2.2 lists tip data. A small laser beam is reflected off the flexible beam, near the tip end, toward a dual-bias photon sensor. The computer takes the sensor's output and returns height profiles during the scanning process. The base of the AFM moves the sample under the AFM tip, providing motion for scanning the surface. The base provides perpendicular fast and slow scan axes for 2-D area height profiling. Figure 2.6 points out some larger components of atomic force microscopes.
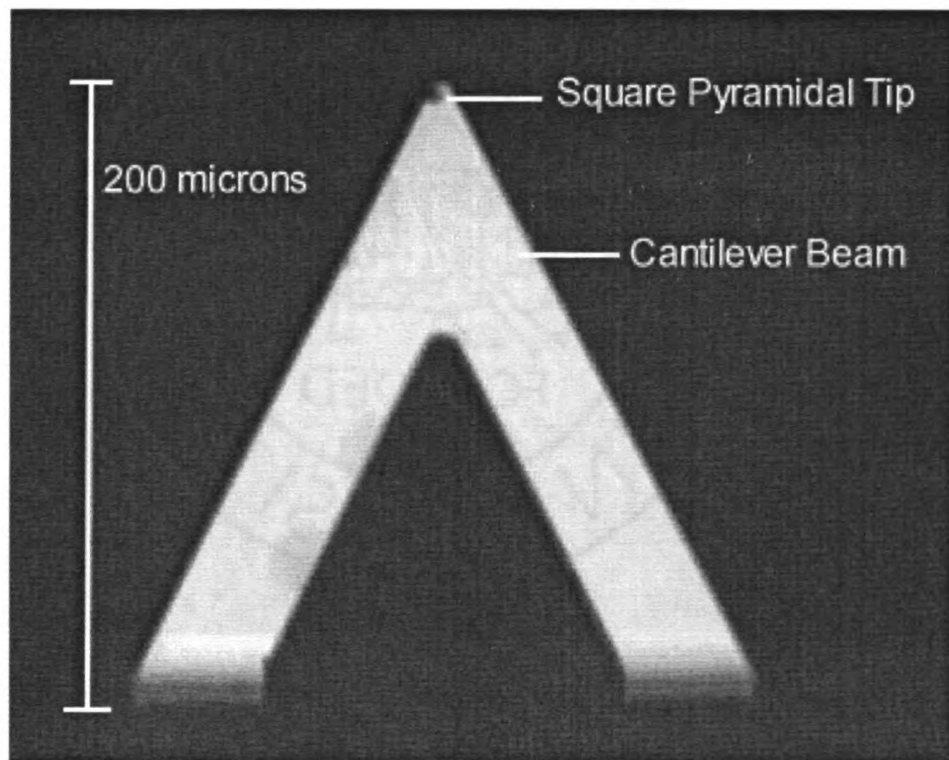
Figure 2.5 Digital Instruments Co. silicon-nitride probe AFM tip

Table 2.2 Digital Instruments Co. standard silicon nitride probe specifications

Spring constant:	0.12 N/m
Tip Radius of Curvature:	20-60 nm
Cantilever Length:	200 μm
Cantilever Configuration:	30° V-shape
Reflective Coating:	Gold
Tip Shape:	Square Pyramidal
Tip Half Angle:	35°
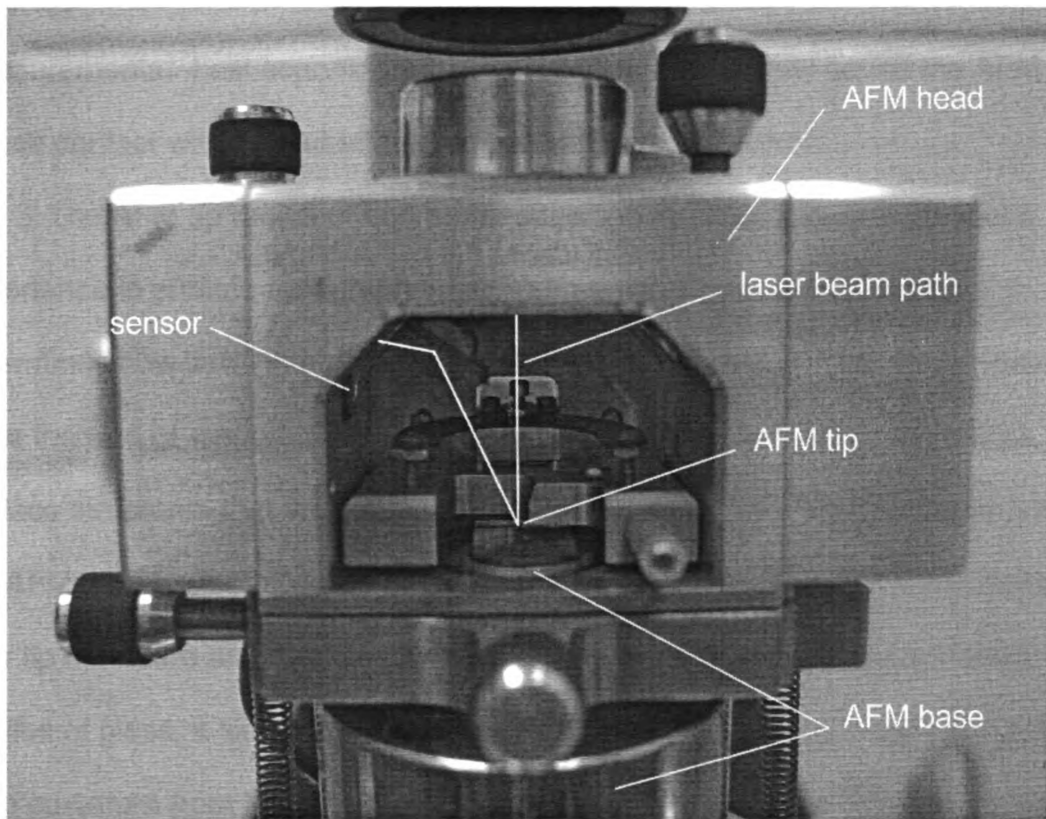
Figure 2.6 Major components of atomic force microscopes

A Digital Instruments Co. Nanoscope III atomic force microscope shown in Figure 2.7 was used in contact mode for profiling surface height of glass specimens. The type-J base was selected to scan areas of 12x12 microns and

smaller. There is also a type-k base that allows scans of approximately 85x85 microns or less. The type J base provided more precise base movement for more accurate surface profiles of small area scans. A sampling rate of 512 samples per scan line was chosen to maximize the profile resolution. The other allowable scan rates are 128 and 256 samples per scan line. A scanning frequency of 6.1 Hz was chosen to minimize the scan time without reducing the accuracy of the surface profiles, since faster scanning rates can skew the height measurements. Fast scanning rates on rough materials may cause the AFM tip to lose contact with the substrate surface and introduce error.

The AFM tip radius of curvature, specified in Table 2.2, is of particular importance in surface topography measurements. The shape of the tip determines how it will interact with the surface it is scanning. The tip curvature limits the size of topographical structures that the AFM can accurately profile. Surface structures that are close to the tip radius or smaller will be distorted in the AFM profile. Atomic force microscopes therefore have resolution limited by their tip curvature and subsequent convolution. When comparing small area profiles of glass, a single tip was used to avoid error in the data from differences in tip curvature from the manufacturer. The tips were found to slowly wear down or collect debris, although the change in RMS roughness measurements on glass were negligible throughout the lifetime use of each tip.

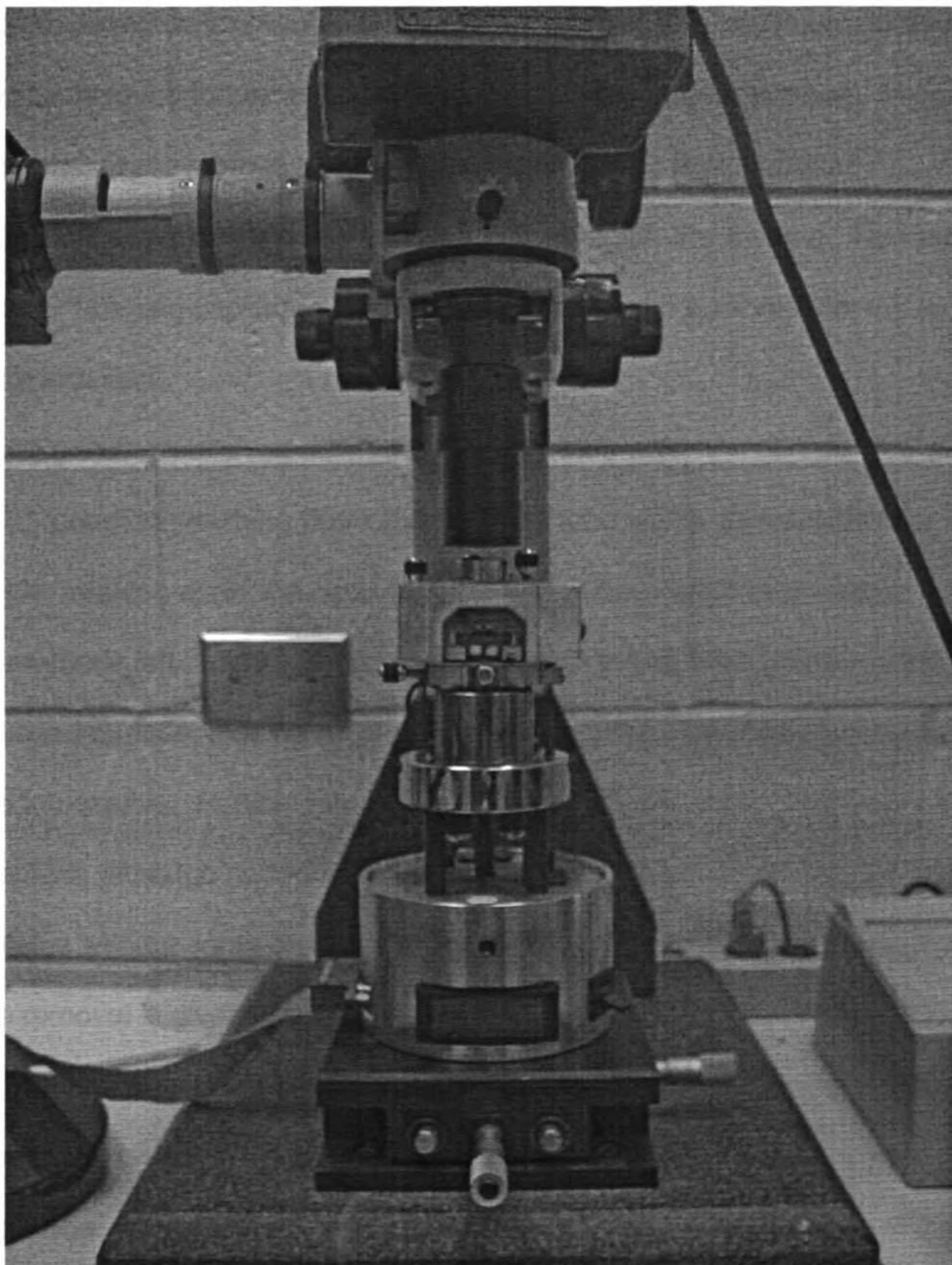Figure 2.7 Digital Instruments Co. Nanoscope III atomic force microscope

2.5.1 Preparation of Capillary Tube Samples

At the beginning of this study, it was apparent that there was little

information available on the interior surfaces of glass capillaries and no standard

techniques available for measuring them. It was therefore necessary to develop our own techniques for accessing and measuring the interior surface. In general, it was necessary to remove half of the capillary tube so that standard measurement instruments could be used to interrogate the surface. Numerous methods of opening capillary tubes were attempted with poor results; these methods included:

(1) grinding/polishing down the capillary tube wall

(2) grinding/polishing down the capillary tube with a dissolvable filler inside

(3) breaking apart the capillary tube with a dissolvable filler inside

These methods left chemical residue or debris on the surface that contaminated the exposed surface, making AFM profiling of an undisrupted capillary tube surface impossible. Particle removal techniques were investigated to overcome this problem, although no techniques guaranteed removal of sub-micron size particulates without some damage to the capillary tube surface. A discussion of particle removal is given in section 1.2.4.

The first step in successfully preparing the capillary tube for the AFM was to remove a short length of the protective plastic coating from around the capillary tube. This ensured a clean break of the glass capillary and produced less chance of the coating being a disruption to the AFM laser beam path, as shown in Figure 2.8. The coating was removed at a point several millimeters from the end of the capillary tube to allow for a grip point when fracturing the tube. One method of removing the plastic coating was tearing it away from the

glass surface with sharp tweezers, although care was taken to avoid crushing the capillary tube.
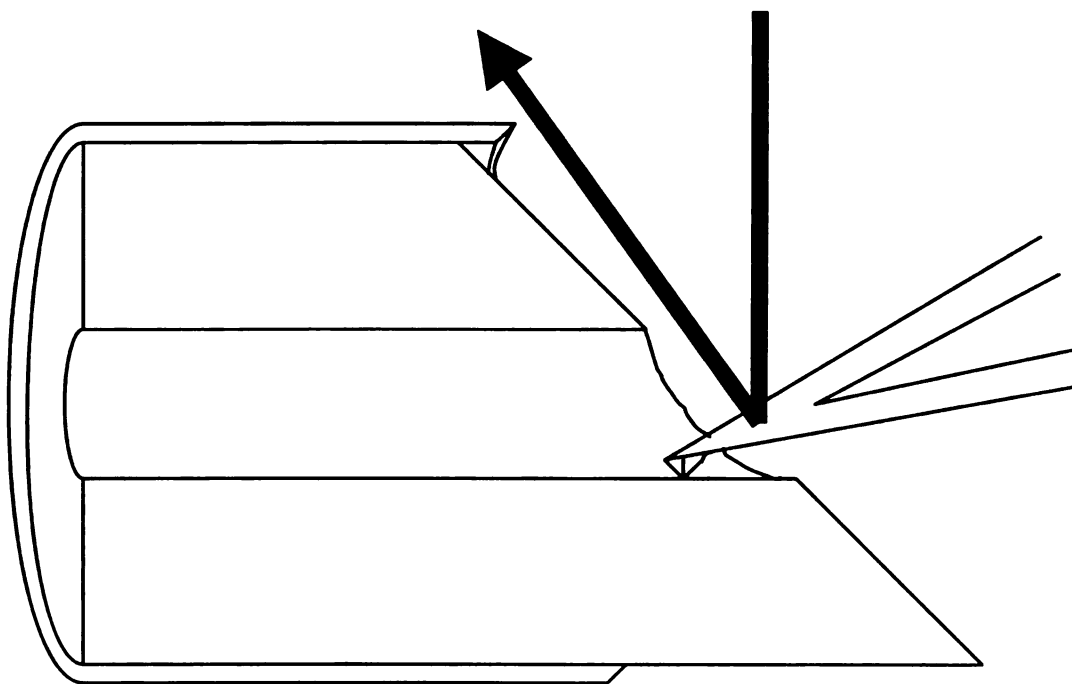
Figure 2.8 Diagram of capillary tube cross-section with an atomic force microscope tip. The arrow shows the laser beam path.

The next step was to place a small scratch in the exposed glass surface to promote a smooth break in the capillary tube. Because of the potential disruption of the AFM laser beam path, the capillary tube needs to have a plane of fracture that exposes as much capillary tube surface as possible. Figure 2.9 shows an image of a capillary tube with a large area of inner surface exposed. A fracture plane perpendicular to the length of the capillary tube will block the path of the laser beam and prevent AFM profiling. A practiced technique was used in producing the proper scratch angle and depth to obtain usable specimens. A

razor blade or a moderately sharp utensil was capable of producing an adequate scratch in the glass surface.
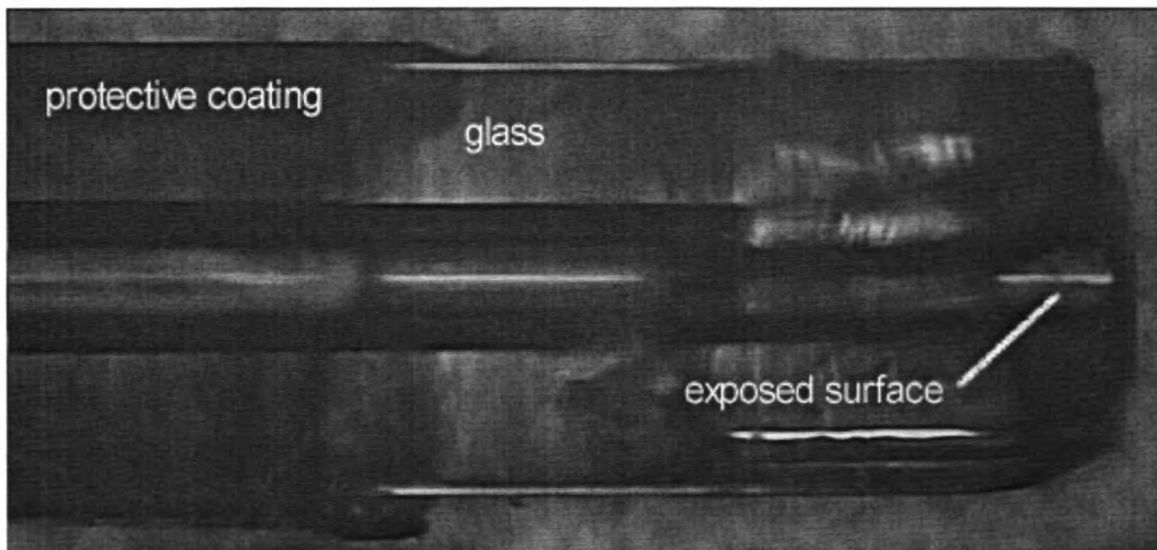
Figure 2.9 Fractured capillary tube with exposed inner surface. 361 μm outside diameter, 75 μm inside diameter.

The fracture of the capillary tube can be accomplished by hand or with tweezers. Applying a bending moment away from the scratch required the least bending force before fracture, while producing the cleanest break through the capillary tube. Compression of the scratch in the capillary tube wall or trying to break the tube without a well defined scratch made the glass more likely to shatter at the fracture site and contaminate the inside of the capillary with debris, often up to several centimeters from the fracture site.

Once a good fracture was produced, as observed by optical microscopy, the specimen was fixed to a ferrous mounting disk. Typical AFM samples have large surface areas, allowing for low strength gel adhesives to be used to mount

the sample to the disk. Capillary tubes have very little surface area for mounting and thus require a much stiffer adhesive to prevent them from moving during AFM profiling. Elmer's™ super glue was chosen for this purpose. The glue was applied to the outer edge of the mounting disk to prevent chemical vapor deposition of the cyanoacrylate onto the exposed surface of the capillary tube. A conservative amount of glue must be used to minimize the glue flow to areas of high surface energy, such as the contact line between the capillary tube and the mounting disk. The capillary tube must be set down through the glue, flat across the disk surface, with the capillary tube surface to be profiled as close to the center of the mounting disk as possible to ensure that the AFM tip can reach it when the disk is mounted in the AFM. A short amount of time was allowed for the glue to set while the capillary tube was held in place. After the glue had set, the excess tube beyond the edge of the mounting disk was broken off to allow the sample to fit inside the AFM sample holder. A prepared capillary tube sample is shown in figure 2.10.
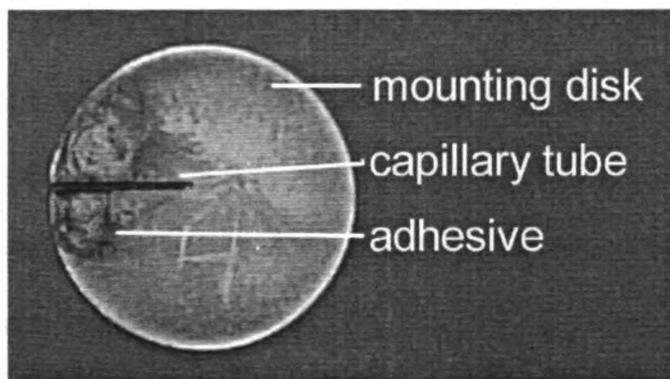

Figure 2.10 Capillary tube attached to a 1.5 cm diameter AFM mounting disk

2.5.2 Profiling Concerns

Care must be taken when attempting to position the AFM tip close to the capillary tube surface as well as during the final computer-controlled approach and subsequent contact of the tip with the glass surface. The sample should be placed to allow proper positioning and contact of the AFM tip inside the capillary. Contact made between the AFM tip and the edges of the capillary tube can contaminate the sample with glass debris and damage the AFM tip. During final computer-controlled approach, the tip was manually centered with the tip position adjusters, to prevent it from contacting the curved edges of the capillary tube. After a successful final approach, slight position adjustments of the tip on the capillary tube wall were be made by mechanical and computer control.

After an AFM profile was captured as a computer file, proper adjustments were made to obtain more accurate measurements of the surface profile. A zero-order "flatten" command was used to remove height jumps between scan lines and curvature perpendicular to scan lines. The flatten command does this by setting the average height of each scan line to zero. A second order "plane fit" command was used to remove curvature in the scan line direction. The plane fit command calculates a second order polynomial from the average curvature of all the scan lines, and subtracts the polynomial from each scan line. With these two fitting functions, the curvature of the capillary tube surface was removed from scans perpendicular and parallel to the capillary tube length. With the curvature removed, surface profiles and roughness statistics of capillary tubes of different diameters could be compared more accurately.

Chapter 3

Experimental Results

3.1   Surface Energy Manipulations
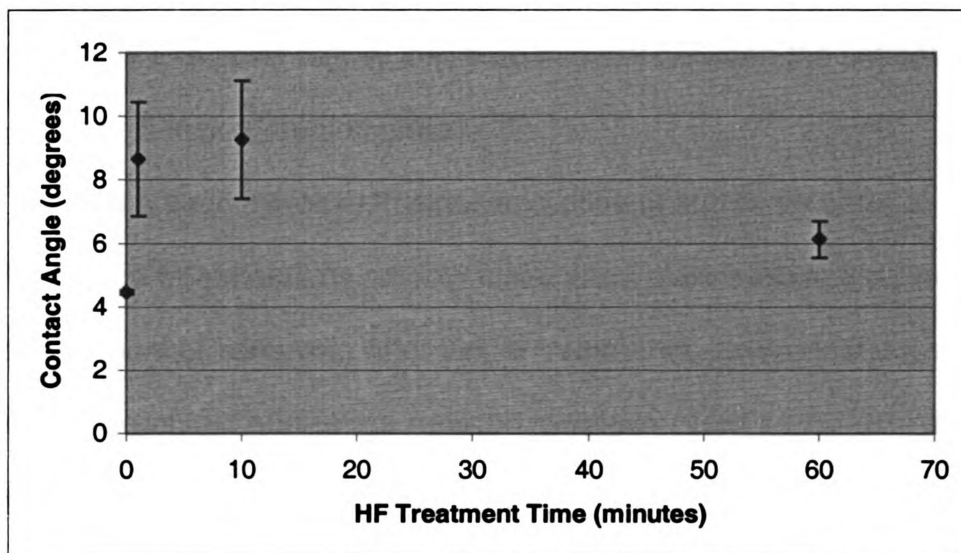
Figure 3.1 Sessile drop water contact angle on pre-cleaned slide glass versus 5% hydrofluoric acid etching time

The data points in Figure 3.1 show the average water contact angle of fused silica glass slides after their respective treatment time in 5% hydrofluoric acid. The length of the error bars represent one standard deviation of the contact angle for each treatment time. The untreated slide had very little variation in contact angles over its surface, as represented by the short length of the error bars. Following 2 and 10 minutes of HF treatment, there was much more variation among the test sites. After 60 minutes of treatment, the contact angle variation diminished.

There is an initial large increase in the contact angle measurements between 0 and 2 minutes of HF treatment times. The contact angle measurements made with the 2 and 10 minute treated slides were similar, between 7° and 11°. The glass treated with HF for 60 minutes shows a reduction of contact angle to a point slightly less than midway between the untreated glass and the 2 and 10 minute treated glass.

There is a large increase in measured contact angles for short duration hydrofluoric acid treatments on smooth fused silica glass surfaces, as well as an increased amount of variance. After longer treatments, the contact angles and variance of the contact angles are reduced to values closer to the untreated glass surface, as seen in Figure 3.1.

Contact angle measurements were also conducted on glass slide surfaces treated with Siliclad™, a monomeric octadecylsilane derivative. The average contact angle was 97.45° with a standard deviation of 1.69°.

3.2   AFM Profiles of Treated Silica Glass
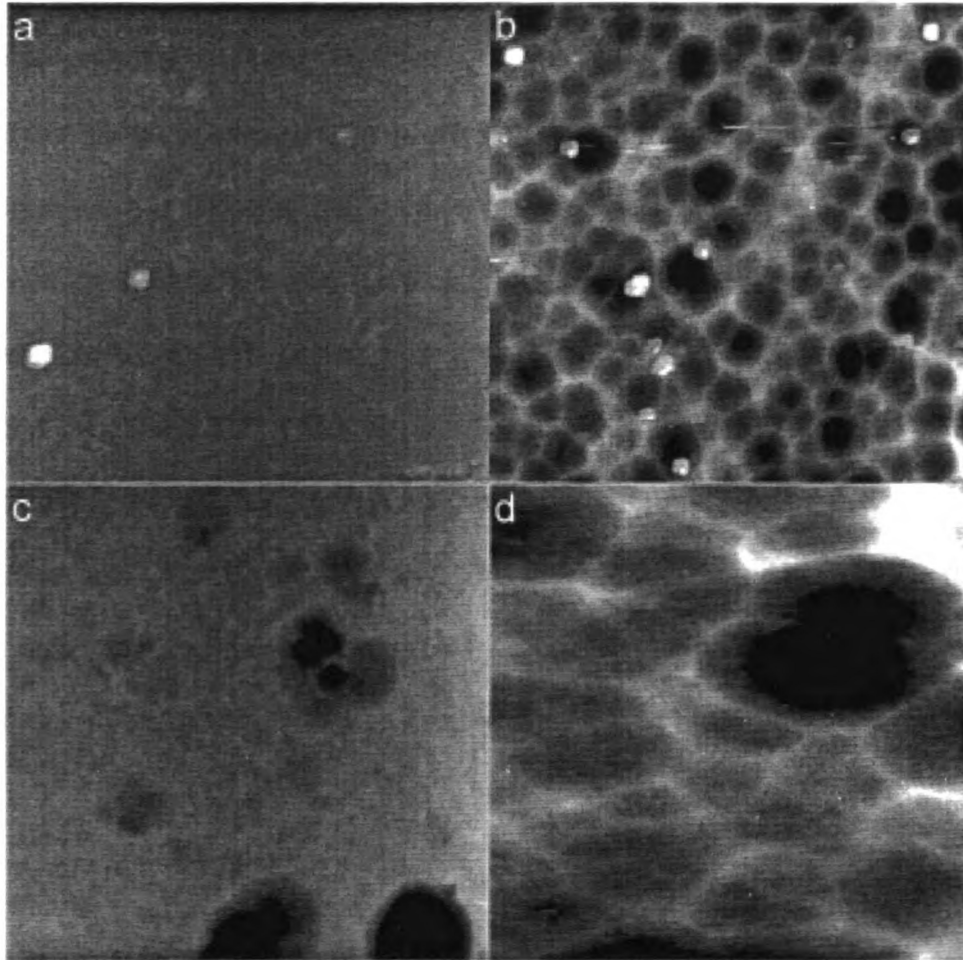
Figure 3.2 AFM 10x10 micron profile images of densely flawed slide glass treated with 5% hydrofluoric acid. (a) untreated (b) 4 minutes (c) 28 minutes (d) 90 minutes.

Figure 3.2 a-d show AFM images of slide glass after four hydrofluoric acid treatment times. The untreated slide is generally featureless, indicating low surface roughness. A visual inspection reveals pitting of the glass surface from the hydrofluoric acid etching. Pits near each other coalesce, resulting in smaller populations of larger pits. Figure 3.3 shows a plot of the RMS roughness of the

slide glass versus hydrofluoric etching time. The roughness of some areas of slide glass is an order of magnitude larger than other areas of slide glass. We term these high and low flaw density areas, respectively. The high flaw density areas of the glass provide a much more irregular surface with inhomogenities, which enhance the physical pitting caused by the chemical etching. Some flaws can be seen under an optical microscope before etching, although the high and low flaw areas on a glass slide are difficult to distinguish between before etching. Figure 3.4 shows the average root-mean-square roughness measurements of higher quality areas of the glass slide for several treatment times in 5% hydrofluoric acid. The error bars represent one standard deviation of the data at each treatment time, centered on the average roughness. There is an increased roughness for the hydrofluoric acid treated slides over the untreated slides.
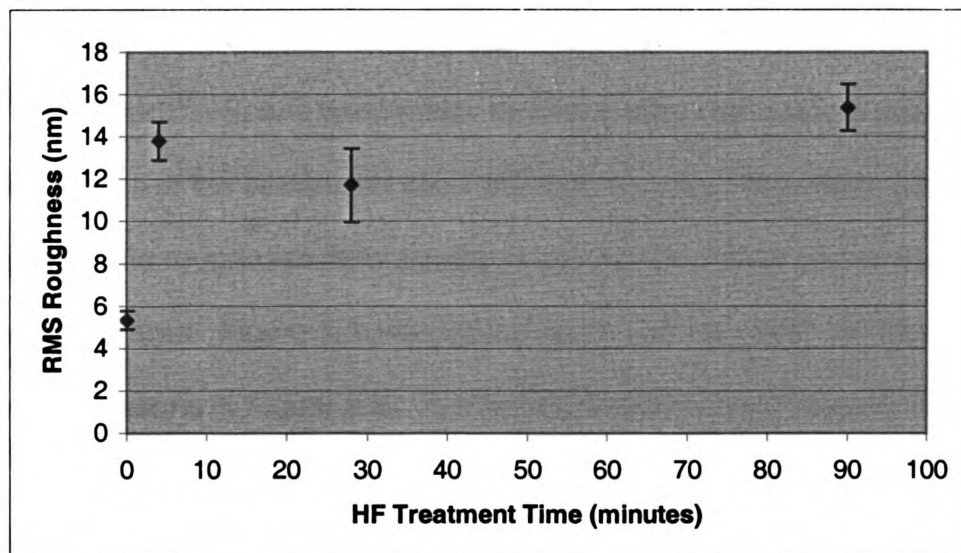
Figure 3.3 AFM 10x10 micron pre-cleaned highly flawed area glass slide RMS roughness versus hydrofluoric acid etching time
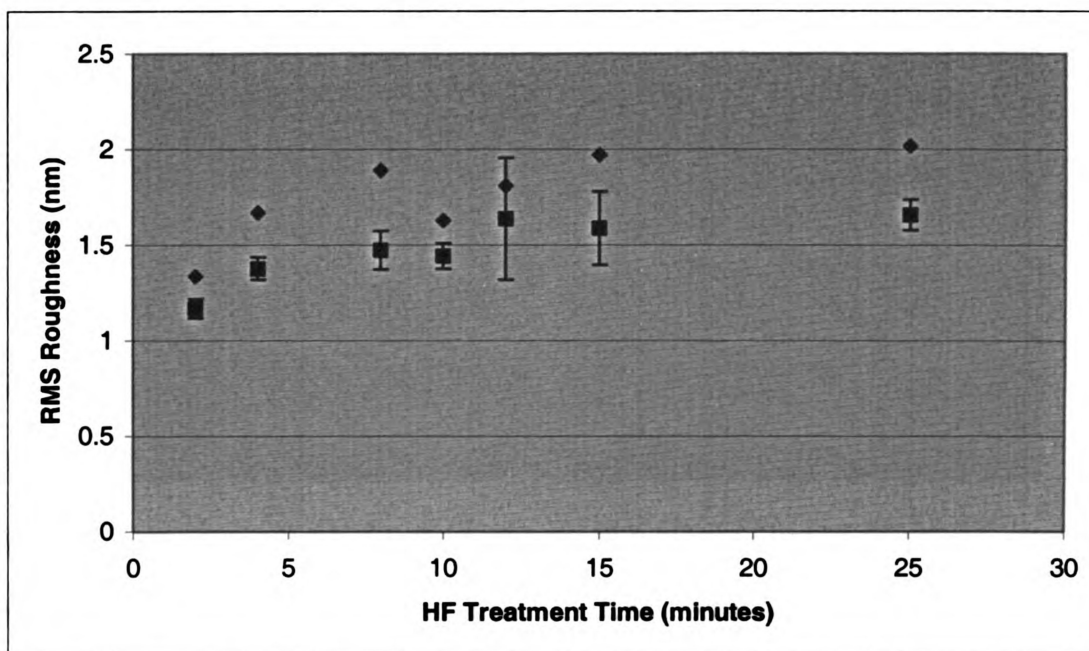
Figure 3.4 AFM 10x10 and 1x1 micron pre-cleaned slide glass RMS roughness versus hydrofluoric acid etching time at low flaw density sites. The error bar lengths are one standard deviation of the data. (diamond) 10x10 micron scan (square) 1x1 micron scans.

AFM profiles were taken on slide glass treated with the hydrophobic silane derivative Siliclad[TM]. Scans were made several times over a single area. The RMS roughness of the siliconized glass surface was seen to reduce sharply after initial scans. The roughness then stayed nearly constant after numerous scans over the same area. Figure 3.5 images are representative AFM profiles of the first and tenth scans in Figure 3.6. The AFM profiles become visually smoother as the number of passes increases over a Siliclad[TM] treated area.
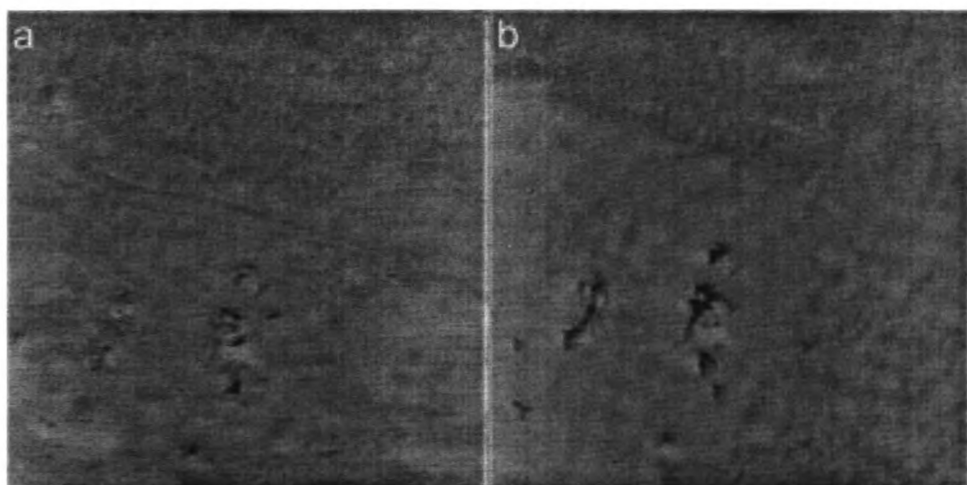
Figure 3.5 4x4 micron AFM profile images of a single area of Siliclad^{TM} derivitized glass surface. (a) first scan (b) tenth scan.
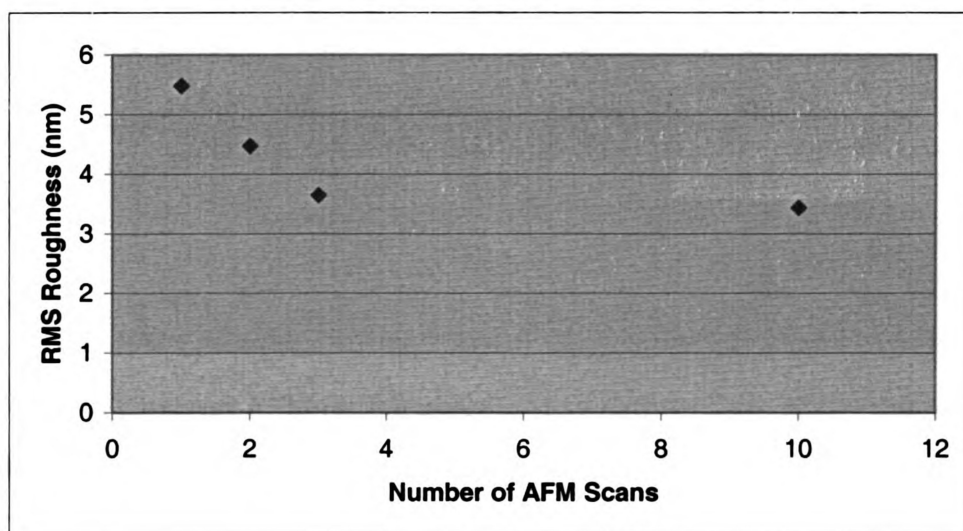
Figure 3.6 AFM RMS roughness of a single 4x4 micron area of Siliclad^{TM} derivitized glass surface versus the number of scans

3.3 AFM Profiles of Capillary Tubes
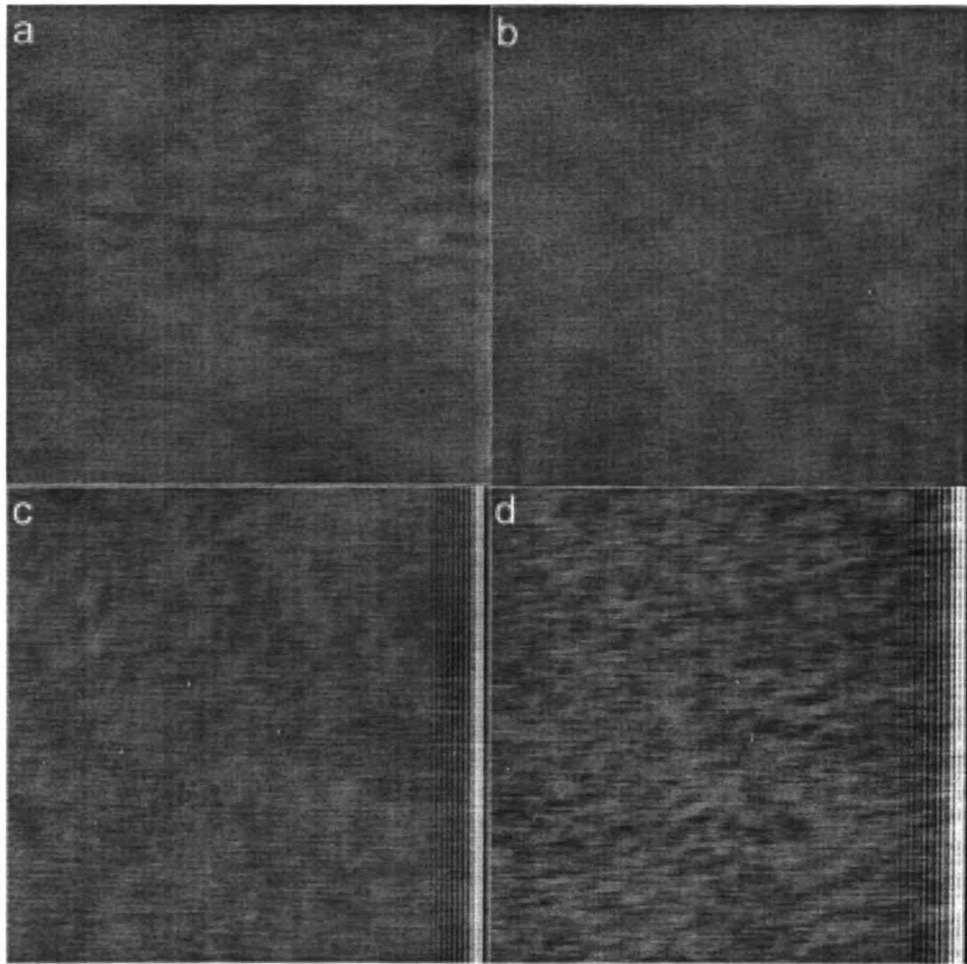
Figure 3.7 1x1 micron AFM profile images of capillary tubes of several inside diameters. (a) 75 microns (b) 100 microns (c) 150 microns (d) 200 microns.

Figure 3.7 a-d shows AFM profile images representative of the surfaces of four different size capillary tubes. Figure 3.8 shows the RMS roughness of 1x1 micron AFM profiles of different size capillary tubes. The data points represent the average roughness. The error bars are one standard deviation of the data for each capillary tube size, centered on the average.

There is a trend of greater RMS roughness for larger capillary tube diameters. It is visually apparent in Figure 3.7 that the 100 micron tube is smoother and the 200 micron tube is rougher than the 75 and 150 micron capillary tubes, with the roughness approximately in proportion to the tube inner diameters.
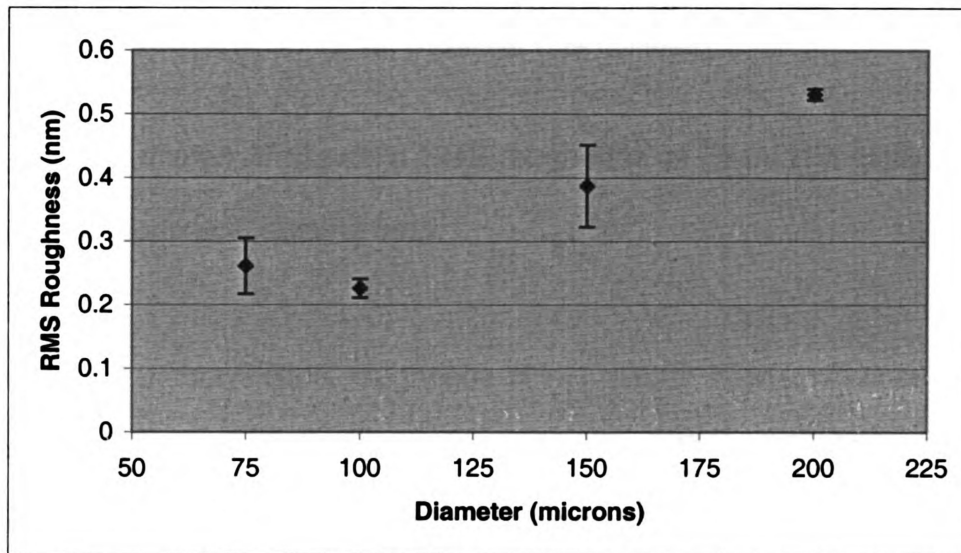
Figure 3.8 1x1 micron AFM profile RMS roughness of capillary tubes versus capillary tube diameter
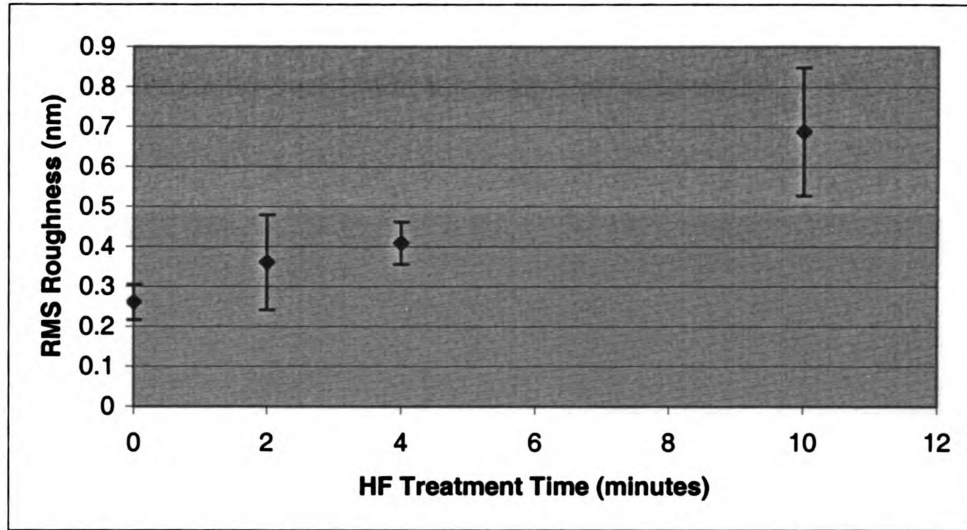
Figure 3.9 1x1 micron AFM profile RMS roughness' of 75 micron capillary tubes versus hydrofluoric acid etching time

Figure 3.9 shows RMS roughness of 1x1 micron AFM profiles of 75 micron ID capillary tubes treated with hydrofluoric acid for several lengths of time. The data points in the figure represent the average RMS roughness. The error bars are one standard deviation of the data at each treatment length.

There is a roughening trend during the HF etching. The data appear to fit a straight line for RMS roughness versus hydrofluoric treatment time. Figure 3.10, a-d are AFM profile images representing the glass surfaces after 0, 2, 4, and 10 minutes in a 5% hydrofluoric acid solution. The glass surface changes from being visually smooth to becoming progressively rougher for longer hydrofluoric acid etching times. Figure 3.10 d shows a great deal of variation in surface roughness across the profile. The top of the profile is very rough, and the bottom is very smooth. This variation is in agreement with the large standard

deviation of the 10 minute etching data in Figure 3.9. The variations in the other

Figure 3.10 profiles also seem to fit the statistical data well.
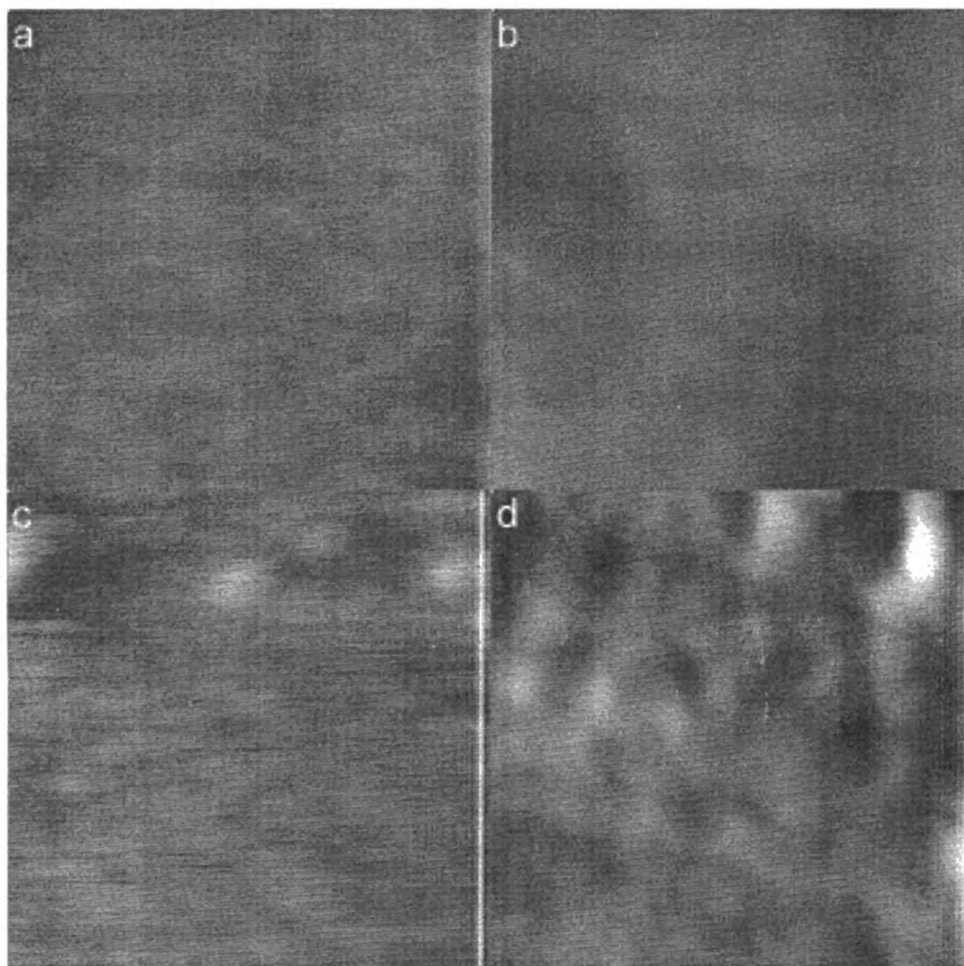
Figure 3.10 1x1 micron AFM profile images of 75 micron inside diameter capillary tubes for several hydrofluoric acid etching times. (a) no treatment (b) 2 minutes (c) 4 minutes (d) 10 minutes.

3.4   Flow Measured Roughness

The results of the flow measured roughness experiment with hydrofluoric acid etched capillary tubes were inconclusive due to lack of data points and problems with the experimentation. The long duration etched tubes showed apparent breakage in several places when observed under an optical microscope. The capillary tubes also seemed to accumulate debris during the etching process, observed in reduced laminar flow rates of etched capillaries over untreated capillaries. The flow measured roughness versus HF treatment data are not presented here because of its lack of application toward the objectives of this investigation.
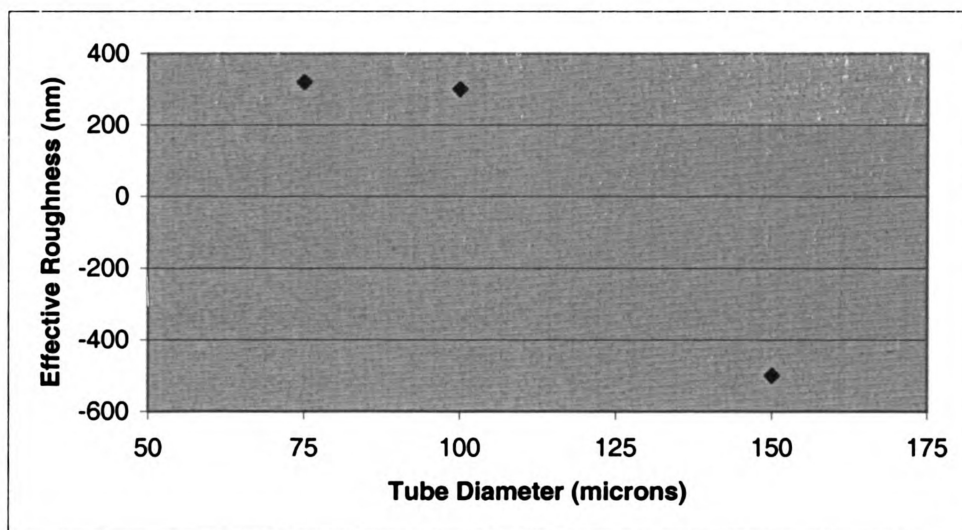
Figure 3.11 Flow measured roughness of untreated glass capillaries versus inside diameter

The results of the flow measured roughness experiments for various sized capillaries are shown in Figure 3.11. A decreasing trend in roughness for

increasing tube diameter can be made, although more data points are needed to confirm this. A negative effective roughness of the 150 μm capillary suggests error in data acquisition or that the empirical equation used to determine the roughness is not accurate under these flow conditions.

Chapter 4

Discussion

4.1   Surface Energy Manipulations

Untreated glass microscope slide surfaces were examined by contact

angle measurements. The measured contact angle of 4.46±0.11° corresponds

closely with values reported in the literature. This value represents a high

surface energy in accord with equation (2.1), or more phenomenological, a

hydrophilic surface. This can be rationalized by considering the chemical nature

of the silica glass surface when exposed to aqueous solutions (as used in our

cleaning conditions) or even laboratory ambient air containing water vapor. The

surface is believed to contain a partial coverage of –OH (hydroxyl) groups bound

to the silicon atoms though dissociation of water molecules. While the standard

deviation of the contact angle is relatively small, indicating that the surface

preparation procedure used can reliably generate a reproducible surface, the

variation in contact angle was found to be dependent upon the part of the glass

slide sampled. This suggests that the surface of the slide is inhomogeneous in

surface composition (-OH concentration) and hence, in surface energy. When

viewed using optical microscopy, no features were visible that could correspond

to the inhomogeneity. The surface was essentially flat and featureless.

The interior surface of the glass capillaries was also examined by optical

microscopy. It similarly showed a featureless surface that was free of defects.

Unfortunately, due to the size constraints of the capillary compared with the size

of a typical water drop in contact angle measurements, it was not possible to

measure the surface energy of the interior of the glass capillary directly. As a result, we must infer the chemical composition of the surface from the glass microscope slides. We have found no evidence that the capillaries and slides behave differently in subsequent experiments.

Several compounds including hydrochloric, hydrofluoric, and sulfuric acid can perform chemical etching of silica glass surfaces. Of these, HF acid is the most widely used compound. In our experiments, both the glass slides and capillaries were treated with the 5% HF solution for various amounts of time and the surface was examined following exposure. For the glass slides, HF etching increased the static contact angle moderately from ~5 to ~9° and then decreased for very long HF exposures, returning to close to the value of the clean surface. Clearly, for short HF exposures, the contact angle indicated a more hydrophobic surface with a correspondingly decreased surface energy. At first glance, the values of static contact angle imply that the HF is chemically modifying the surface of the slide, perhaps by exchanging –OH groups for F. Since a fluorinated silica surface is typically more hydrophobic than pure silica, for example the inertness of Teflon, this would produce the higher contact angles and deviation in the data for the initial hydrofluoric acid treatment of the slide glass in Figure 3.1. However, such an effect would be expected to continue to increase the hydrophobic nature of the surface, even for very long HF treatment times. The decrease in contact angle observed in the data of Figure 3.1 suggests that another effect is also contributing to the increased surface energy at very long (up to 60 minutes) etching times.

Optical microscopy indicates that severe changes in the surface roughness take place during HF etching. Dense groups of small defects covered about 50% the glass surface and became visible under an optical microscope after a few minutes of etching. It is known that static contact angle measurements become unreliable on roughened surfaces since the surface energy of a rough surface is intrinsically higher than a smooth surface of identical composition. As explained previously, advancing and receding contact angle measurements can be made to partially compensate for rough surfaces, but these were not successful in our case probably because of gases trapped in the cavities created during etching. This effect produces a very inhomogeneous surface after etching.

Although we have no direct evidence for the presence of defects on the untreated glass surface, either from optical or AFM images, it has been speculated that very small defects act as the initial sites of attack by HF on silica (Spierings 1993). During the initial etching process, the defects are likely to become cavities. For hydrofluoric acid etching, the glass inside the cavities may become partially fluorinated or have adsorbed fluorine compounds. Etching by-products, for example H_2SiF_6 (Spierings 1993), may be adsorbed inside the cavities and accumulate. As such, cavities may develop a surface chemical composition that is considerably different to the unetched regions of the slide. After long etching times, the slide glass cavities grow wider and coalesce, eventually eliminating all of the original unetched surface, and making for a more homogenous surface with decreased contact angle. The observed decreases in

contact angle between 10 and 60 minutes cannot be entirely due to measurement artifacts produced by changes in surface roughness since Figure 3.3 indicates that the roughness is essentially constant during this time. The changes in contact angle may be due to reduced concentrations of fluorine on the glass surface after long periods of etching.

The contact angles measured for Siliclad™ treated glass slides were similar to published data from the manufacturer. The addition of the aliphatic molecule to the silica surface increases the contact angle to about 90°. This is consistent with replacement of some of the original surface –OH groups by the long chain hydrocarbon portion of the octadecylsilane derivative. The surface of the glass effectively becomes terminated with $-CH_3$ groups of the chain. These methyl groups, as well as the rest of the hydrocarbon chain, interact very weakly with water molecules and generate the observed nature of a low surface energy/non-hydrophilic surface.

To ensure that the alkylsilane molecule only affects the chemical composition of the surface and not the topography, optical microscopy was performed and confirmed no major changes. In addition, AFM images were acquired and produced RMS roughness values almost identical to the untreated surface. However, the RMS roughness was observed to decrease with continued scanning of the AFM tip. This observation indicated motion of the alkylsilicone molecules on the derivitized glass surface. The chain of molecules that make up the hydrophobic coating seemed to be mobile and apparently "flattened" the surface, eventually reaching an RMS roughness of about 3.4 nm

after 3-4 scan passes, as seen in Figure 3.6. It seems likely that the tip may also

pick up loosely adsorbed alkylsilanes, further complicating the measurement of

the true surface roughness.

As before, although we could also Siliclad™ treat capillaries,

measurements of contact angle were not possible. In light of the effects of the

alkylsilane on the clean glass slides, we must infer a similar effect on the

capillaries: an increasingly hydrophobic surface with little change in surface

roughness.

4.2   Surface Roughening by Hydrofluoric Acid

Affatigato et al (1996) reported a rapid initial roughening trend with HF

treatment for slide glass. The rate of roughening became slower and almost

linear after about 10 minutes of etching. Affatigato et al (1996) also found that

rougher initial surfaces created larger rates of roughening during the first several

minutes of etching. This trend was also seen in our hydrofluoric acid etched slide

glass as indicated in Figures 3.3 and 3.4. The rapid roughening of the glass slide

that contained a high concentration of visible flaws or defects (Figure 3.3) was

greatly reduced for a slide that contained a low concentration of flaws (Figure

3.4). This supports the hypothesis that defects are the initial sites of attack by

HF and that the defect-free surface is etched only slowly. The ultimate rate of

roughening seems independent of the initial condition of the glass.

Another characteristic of hydrofluoric acid etched glass has also been

identified in literature. Tso et al (1982), Spierings (1993), and Affatigato et al

(1996) counted progressively fewer flaws per unit area during the hydrofluoric acid etching. This effect is also seen in our data of Figure 3.2. As mentioned above, the mechanism for HF roughening appears to be focused initially at intrinsic defects that enlarge and gradually coalesce. Once the cavities coalesce and their edges begin to touch, the measured RMS roughness is approximately constant.

The RMS roughness of the untreated capillary tubes appears to be slightly smaller than the untreated glass slide (Figures 3.4 and 3.8). It is certainly true that the small capillaries tend to have smoother inside walls than the larger ones. For example, the RMS roughness of the 200 micron capillary is about 0.5 nm while the 75 micron capillary is about 0.25 nm. Presumably, these features are a result of the manufacturing processes. The tubes are drawn over a mandrel at elevated temperature when the silica is soft. The capillaries have identical outside diameters and so the 75 micron inside diameter tubes have much thicker walls than the 200 micron tubes. This may result in slower cooling rates for the smaller inside diameter tubes, allowing some degree of annealing during the cooling period.

Unlike flat slide glass, the roughness of the inside wall of the capillary increases at an approximately linear rate throughout the etching process, as shown in Figure 3.9. Unfortunately, it was not possible to extend the HF treatment time beyond 10 minutes due to disintegration of the capillary, so we are unable to determine if a plateau roughness is reached, as is it for the slides. It is worth noting that the absolute roughness of the capillary glass after ten

minutes of etching is about a factor of two less than the flat slide, although differences in the way the etching was performed make direct comparison difficult. It was expected that smoother surfaces would roughen slower, since it is flaws in the surface that provide more surface area for rapid etching and initial roughening of the silica glass over the slower, kinetically-controlled dissolution rate of very smooth unflawed glass (Spierings 1993).

4.3   Comparing Capillary Tube and Slide Glass Surfaces: Towards a Model Surface

The less flawed areas of the glass slides provided better models of capillary tube surface when compared to areas of higher flaw densities, though the slide glass RMS roughness in the most unflawed and homogeneous areas is over twice the RMS roughness of the roughest untreated capillary tube. A prominent linear trend of increasing roughness versus hydrofluoric acid etching time seems applicable to both the slide glass, Figure 3.4, and the 75 micron capillary tubes, Figure 3.9. A linear trend is not seen for the higher flaw density areas of slide glass shown in Figure 3.3. In an attempt to find a better model of the capillary tube surface, the RMS roughness of untreated quartz glass was also measured to be more than twice as large as the roughest untreated capillary tube. A higher quality fused silica or quartz glass may be necessary to more accurately model surface treatments of capillary tubes on flat surfaces. Alternatively, annealing the slide glass at temperatures close to the softening point may reduce the roughness of its surfaces.

4.4   Flow Measured Roughness

In small pipes, such as capillary tubes, the viscous sub-layer thickness is reduced to the radius of the pipe. This constraint makes a larger length ratio of equivalent roughness height to the viscous sub-layer thickness; effectively making flow measured roughness more accurate than for larger pipe diameters. Although, roughness measurements of glass surfaces become more precise in capillary tubes, the experiments are likely to have determined the microscale roughness of the tube and not the nanoscale roughness of the tube walls. Most of the pressure drop, assigned to surface roughness of the capillary tubes, might occur from large-scale variations in the surface of the capillary tubes. The nanoscale roughness of the tube walls probably had a much smaller effect on the pressure drop across the capillary tube than the microscale fluctuations in capillary tube diameter, cross-sectional area, and roundness. Therefore, flow measured roughness does not seem promising for future roughness measurement correlation with nucleation thresholds in capillary tubes.

4.5   Consequences for Nucleation Studies

The major motivations and interests in this study were to investigate how silica glass surface properties relate to nucleation thresholds and to find ways of effectively manipulating these surfaces to influence the thresholds. Both hydrofluoric acid etching and octadecylsilane derivatization effectively manipulated the surface properties of the glass. Although their effects of

48

influencing nucleation thresholds have not been studied, the silane and etching treatments' influence on nucleation thresholds should be predictable.

The hydrocarbons form a long chain starting at the silane bond to the glass surface. The hydrocarbons seem to be freely mobile, as shown in Figure 3.5. The loose packing and hydrophobic nature of the hydrocarbon chains are likely to produce pockets of trapped gases when the derivitized surface is exposed to aqueous solutions. Trapped gases, as well as hydrophobic crevices are known to reduce nucleation thresholds in water (Atchley et al 1989).

Hydrofluoric acid etching has been theorized, in section 4.1, to initially produce moderately hydrophobic cavities in glass. The initial glass etching should also reduce nucleation thresholds by providing hydrophobic crevices and possibly trapped gases in these crevices. For long duration etching, the glass may have slightly increased nucleation thresholds over slightly etched surfaces. This is predicted because the contact angle is reduced and the surface roughness stays nearly constant relative to the slightly etched silica glass measurements, as seen in Figures 3.1, 3.3, and 3.4.

The predictions of the changes in nucleation thresholds for silica glass should also apply to capillary tubes, although the extent of these changes is not easily predicted. The nucleation thresholds seem to be mostly a factor of the evaporating space available in the capillary tubes. This would suggest that changing the surface might do little to affect bubble growth in confined volumes, although nucleation points in capillary tubes may actually vary more substantially on the topography and energy of their surface since their nucleation thresholds

are raised very high above normal surface thresholds. Nucleation threshold

experiments in capillary tubes should help to determine the extent of which

surface properties are involved.

Chapter 5

Concluding Remarks and Recommendations

In this thesis, the need for investigation of the surface properties of glass capillaries was addressed. Techniques to successfully profile the surface of capillary tubes were defined. Roughness of capillary tube surface was modified and measurable with consistency. The research performed here should allow designing of glass surfaces to promote or inhibit bubble formation by altering the chemistry or topography of the surfaces.

Due to the limited time frame of this research, several ideas have been suggested for further investigation;

- High quality fused silica or quartz glass should be tried as a model for capillary tube glass. Although measurements of the surface topography inside capillary tubes were successful, it may be easier to perform surface measurements on flat model surfaces.

- Since surface tension measurements were not done in capillary tubes, the use of capillary rise to measure the surface tension of treated capillary tubes, or a picture of the meniscus of fluid inside the capillary tube for contact angle measurement, should be done to further this research.

- X-ray photoelectron spectroscopy of hydrofluoric acid treated glass should be done to see how much fluorine is left on glass surfaces after etching. This would help in characterizing the effects of etching.

- Nucleation tests should be done on altered capillary tubes to determine the inhibition or promotion that treatments have on bubble formation.

Bibliography

[1]   Adamson, A. W., 1990, *Physical Chemistry of Surfaces*, fifth edition, (John Wiley and Sons, Inc.) pp. 379-400

[2]   Affatigato, M., Osborne, D., and Haglund, R. F. Jr., 1996, "Effect of Surface Roughness on the Acid Etching of Amorphous Silica," *Journal of the American Ceramic Society*, 79 [3], pp. 688-94

[3]   Atchley, A. A., and Prosperetti, A., 1989, "The Crevice Model of Bubble Nucleation," *Journal of the Acoustic Society of America*, 86 [3], pp. 1065-1084

[4]   Brereton, G. J., Crilly, R. J., and Spears, J. R., 1998, "Nucleation in Small Capillary Tubes," *Chemical Physics*, 230, pp. 253-265

[5]   Carey, V. P., 1992, *Liquid-Vapor Phase Change Phenomena*, Hemisphere Publishing Co.

[6]   Ghosh, A., and Ryszytiwskyj, W. P., 1995, "Removal of Glass Particles from Glass Surfaces: A Review," In *Particles on Surfaces*, (New York: Marcel Dekker, Inc.) pp. 353-362

[7]   Jang, H. K., Chung, Y. D., Whangbo, S. W., Lee, Y. S., Lyo, I. W., Whang, C. N., Lee, S. J., and Kim, G., 2000, "Effects of Chemical Etching with Sulfuric Acid on Glass Surface," *Journal of Vacuum Science and Technology A*, 18 [2], pp. 401-404

[8]   Jang, H. K., Chung, Y. D., Whangbo, Y. S., Lyo, I. W., Whang, C. N., Lee, S. J., and Lee, S., 2000, "Effects of Chemical Etching with Hydrochloric Acid on Glass Surface," *Journal of Vacuum Science and Technology A*, 18 [5], pp. 2563-2567

[9]   Liu, X., 2001, *Nucleation of Gas-Supersaturated Liquids*, a dissertation, Michigan State University, University Microfilms, Inc.

[10]   Munson, B. R., Young, D.F., Okiishi, T. H., 1998, *Fundamentals of Fluid Mechanics*, third edition, (John Wiley and Sons, Inc.) pp. 459-508

[11]   Peng, X. F., Hu, H. Y., and Wang, B. X., 1998, "Boiling Nucleation During Liquid Flow in Microchannels," *International Journal of Heat and Mass Transfer*, 41 [1], pp. 101-106

[12]   Peng, X. F., Tien, Y., and Lee, D. J., 2001, "Bubble Nucleation in Microchannels: Statistical Mechanics Approach," *International Journal of Heat and Mass Transfer*, 44, pp. 2957-2964

[13]   Spierings, G. A. C. M., 1993, "Review: Wet Chemical Etching of Silicate Glasses in Hydrofluoric Acid Based Solutions," *Journal of Materials Science*, 28, pp.6261-6273

[14]   Tso, S. T., and Pask, J. A., 1982, "Reaction of Glasses with Hydrofluoric Acid Solution," *Journal of the American Ceramic Society*, 65 [7], pp. 360-362